

Application of the Unsteady Numerical Method of Godunov to Computation of Supersonic Flows Past Bell-Shaped Bodies

THOMAS D. TAYLOR AND BRUCE S. MASSON

Northrop Corporate Laboratories, Hawthorne, California 90250

Received November 11, 1969

The unsteady numerical method of Godunov has been applied to compute high Mach number axisymmetric flow past bell-shaped bodies of varying bluntness. For this configuration the shock layer is governed by the inviscid flow of gas with an embedded contact surface and shock wave. These discontinuities arise from the triple point interaction between the oblique bow shock from the forebody with the near normal skirt shock generated by the flare at the rear of the profile. In the numerical computation, both of these shocks are maintained as discrete discontinuities. The internal flow discontinuities are treated implicitly, however. The results obtained for an ideal gas flow with a free stream Mach number of 8.0 are shown. Included are the positions of the bow shock, secondary shocks, and sonic line, as well as pressure distributions. The shock positions and pressure distributions are compared with experiments. The comparisons are used to assess the limitations of the method.

INTRODUCTION

Presently, the trend of technology is toward development of bodies for reliable flight at supersonic and hypersonic speeds. As a result, there is an increasing need for methods to accurately calculate aerodynamic flow past complex body shapes in these velocity regimes. Current methods are known which give reasonable results for inviscid flow provided the body of interest produces small gradients in the shock layer. These include unsteady calculations by the method of Lax-Wendroff [1] as employed by Burstein [2], the method of Rusanov [3], the method of Godunov [4] as employed by Masson, Taylor, and Foster [5] and the method of Moretti and Abbott [6]. The steady calculation methods include the integral technique of Dorodnitsyn [7] as applied by Belotserkovskii [8] and the finite difference method of Gilinskiy, Telenin, and Tinyakov [9]. If a body has large changes in curvature, which is typical of many practical cases, the dependability of existing methods becomes an open question. In order to establish a reliable approach to computing flows with large gradients the authors undertook the study reported in this paper.

In selecting the computing method the authors relied on studies [4, 5, 10] which indicated that the Godunov finite difference method produced accurate results for smooth flows and, in addition, was optimal for computing smoothly through shock waves. Since the gradient in a flow will be a maximum at a shock wave it was concluded that the Godunov method should be dependable for computing flows past bodies with large curvatures.

After selecting the method the authors attempted to optimize the flow calculation procedure. In order to reduce shock smearing as well as calculation points the authors followed Godunov's original approach and employed the bow shock as the outer grid boundary and explicitly computed its position. Shock waves internal to the grid were smeared, however. The remaining boundaries of the grid were chosen as the body, the axis of symmetry and a plane connecting the bow shock and body in the downstream supersonic flow. The location of the downstream boundary does not affect the flow upstream provided it is in the supersonic region.

Within the prescribed boundaries the inviscid flow equations were differenced by Godunov's method, which is described briefly in technical discussion. The resulting unsteady difference equations were then integrated forward in time from a prescribed initial flow to a steady condition. The initial flow was chosen to be a linear distribution of variables along rays between the bow shock and the body. On the body Newtonian flow was assumed while at the bow shock the flow was calculated from the free stream conditions and the shock wave relations.

The selection of the geometry for testing the method was made with the requirement that both strong expansions and compressions be present. In this connection the authors chose to study flows past bell-shaped bodies. This shape provides an optimum test of the method since it has both convex and concave curvatures. The one difficulty with such a shape is that viscous effects can become important and, in some instances, totally determine the flow pattern. This is shown clearly in the experimental work of Jones, Bushnell, and Hunt [11]. The exact conditions for which viscous effects dominate the flow presently are not fully understood. The experiments indicate, however, that the viscous influence on the shock pattern decreases as the free stream Reynolds number increases and consequently at high Reynolds number ($> 10^6$ based on the maximum body diameter) inviscid flow calculations can be uncoupled from the viscous calculations to a first approximation. The inviscid calculations presented in this paper therefore are of practical use only for the large Reynolds number conditions.

The test calculations were conducted on two bell-shaped bodies, each of which generates strong compression waves near the surface and triple point shock conditions at the bow shock. The test were made for Mach 8 flow conditions with an ideal gas. The value of the adiabatic gas constant, γ , was chosen to be 1.4. The procedure used to make the calculations and the results will now be discussed.

TECHNICAL DISCUSSION

The equations used to describe the inviscid flow were employed in the form

$$f_t + G_x + H_y + y^{-1}Q = 0 \tag{1}$$

where the quantities f , G , H , and Q are the vector functions

$$f = \begin{bmatrix} \rho \\ \rho u \\ \rho v \\ \rho E \end{bmatrix}, \quad G = \begin{bmatrix} \rho u \\ \rho u^2 + p \\ \rho uv \\ \rho uE + pu \end{bmatrix},$$

$$H = \begin{bmatrix} \rho v \\ \rho uv \\ \rho v^2 + p \\ \rho vE + pv \end{bmatrix} \quad \text{and} \quad Q = k \begin{bmatrix} \rho v \\ \rho uv \\ \rho v^2 \\ \rho v(E + p/\rho) \end{bmatrix}$$

In these relations $k = 0, 1$ for plane or axisymmetric flow, respectively and $E =$ internal energy + kinetic energy $= e + \frac{1}{2}(u^2 + v^2)$.

The mesh system for the shock layer is shown in Fig. 1. The cell coordinates are formed by first introducing a set of rays which are approximately normal to the body surface. Each ray is characterized by the angle, θ_i , which it forms with the axis of symmetry. Each ray is then divided into equally spaced segments between

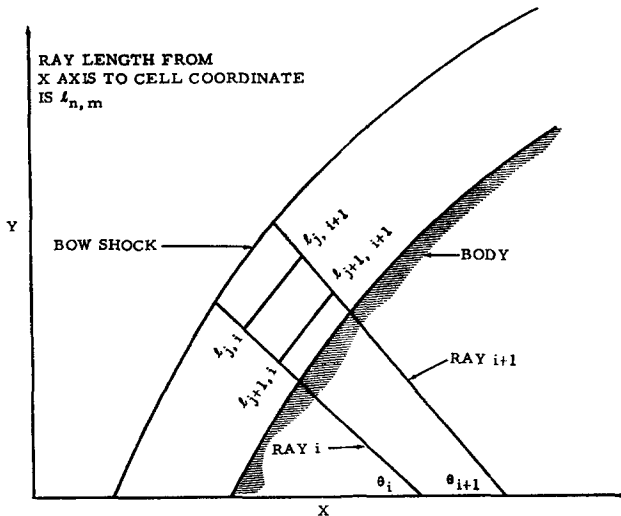


FIG. 1. Coordinate system for calculation.

the body and the bow shock. The distance along the ray, i , from the axis of symmetry to the cell coordinate, j , is denoted by $l_{j,i}$. The difference equations for each cell are derived by integrating Eq (1) over the volume of the cell. The resulting expression can be written in the form

$$\frac{\Delta_t(\mathbf{f}_{\langle i,j \rangle} A)}{\Delta t} + \Delta_t(\bar{\mathbf{H}}s)_{\langle j,t \rangle} + \Delta_j(\bar{\mathbf{H}}s)_{\langle i,t \rangle} + (QA/y)_{\langle i,j,t \rangle} = 0 \tag{2}$$

where

$$\bar{\mathbf{H}} = \begin{bmatrix} \rho(q_n - V_n) \\ \rho u(q_n - V_n) + p \sin \theta \\ \rho v(q_n - V_n) + p \cos \theta \\ \rho E + p \end{bmatrix}, \quad \Delta_\nu \mathbf{f} = \mathbf{f}_{\nu+1} - \mathbf{f}_\nu \quad \text{for } \nu = i, j, t$$

and the symbol $\langle i, j \rangle$ denotes the average over the interval i to $i + 1$ and j to $j + 1$ defined by $\mathbf{f}_{\langle i,j \rangle} = \iint \mathbf{f} dx dy / A$. Similarly the symbol $\langle j, t \rangle$ denotes the average over the intervals j to $j + 1$ and Δt . For the boundary under consideration the quantity q_n denotes the velocity of flow normal to the boundary and V_n is the normal velocity at which the boundary is moving. A is the area of the mesh element and s is the arc length of the boundary under consideration.

The finite difference equations describe the behavior of the space averaged flow variables, $\mathbf{f}_{\langle i,j \rangle}$, in each cell. In order to solve the difference equations, however, it is necessary to relate the values of the boundary fluxes, $\mathbf{H}_{\langle j,t \rangle}$ and $\mathbf{H}_{\langle i,t \rangle}$, to the averaged cell flow variables, $\mathbf{f}_{\langle i,j \rangle}$. The basic concept for relating these quantities was proposed by Godunov. The procedure is to consider each boundary of a cell as a one dimensional initial value (Riemann) problem and utilize the averaged flow quantities of the cells on each side of the boundary for the initial states. The value of the flux $\mathbf{H}_{\langle i,t \rangle}$ or $\mathbf{H}_{\langle j,t \rangle}$ is then determined in the following manner.

First, the one dimensional problem is posed so that the cell boundary is the reference point for all waves resulting from the initial discontinuity. The typical wave pattern is shown in Fig. (2). Next the strengths and velocities of the waves are calculated from relationships derived by Godunov [10]. From this information

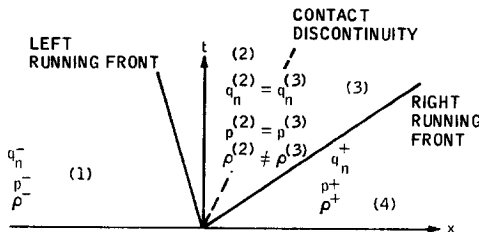


FIG. 2. Evolution of Discontinuity in Fluid State.

it is then possible to determine the location of the cell boundary with respect to the positions of the waves.

The general computation procedure was carefully checked on flows past smooth bodies before attempting the calculations reported in this paper. A portion of the results appear in reference [5].

DISCUSSION OF RESULTS

Two bell-shaped bodies were selected to test the numerical method. The first was a blunt bell with a nose radius of $4/10$ the base diameter. The body, along with the rays of the mesh, are shown in Fig. 3. This case was chosen for two reasons. First the flow would result in a triple point along the bow shock, but the angle between the two branches of the bow shock near the triple point would not approach

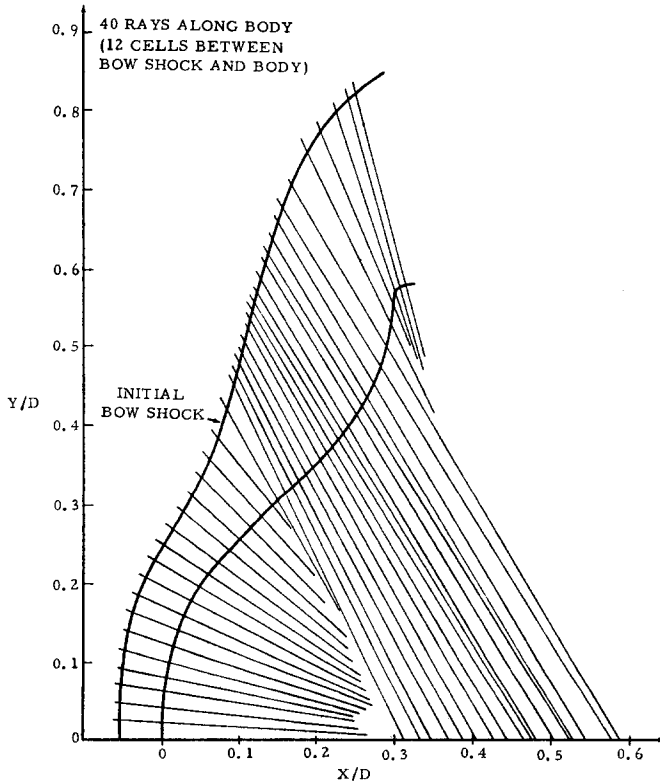


FIG. 3. Mesh rays and initial bow shock shape for body 1.

ninety degrees. Secondly, the interior shock stem from the triple point interacts with the sonic line of the flow. Each of these conditions introduce singularities in the flow which traditionally cause numerical computations to become unstable if one seeks accuracy or very smeared if one attempts to keep the calculation stable.

The flow past body 1 was computed for a Mach 8.0 free stream with 12 cells between the bow shock and the body and 40 rays along the body. In order to reduce computation time the calculation was carried out in two steps. First a very crude bow shock shape was assumed and the flow was computed for 300 time steps. This is approximately the time required for the flow to travel one body length. The bow shock was then smoothed and the calculation restarted. This smoothed bow shock is shown in Fig. 3. The resulting shock and sonic line patterns after the flow become steady to three significant figures (1200 time steps from the restart) are shown in Fig. 4. Note the position of the sonic line in the nose region of the body. As in most cases the flow becomes supersonic along the bow shock, but for this

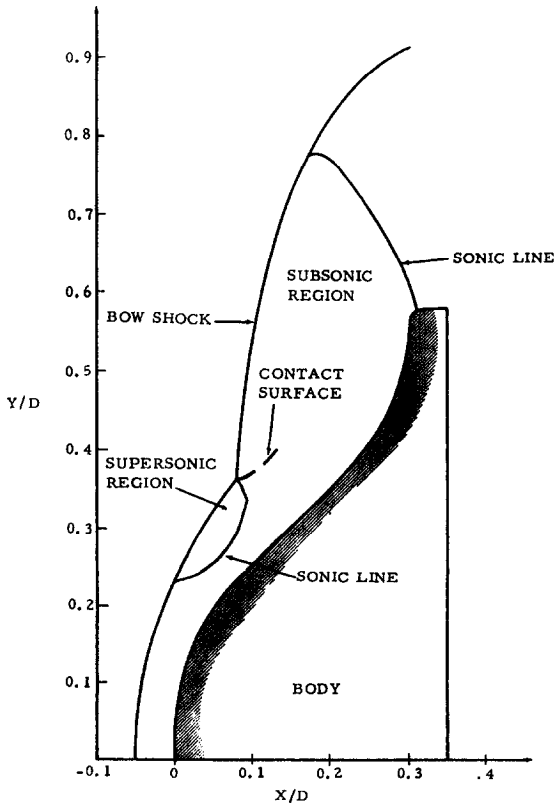


FIG. 4. Bow shock and sonic line position for mach 8.0 flow past body 1 after 1200 time steps.

problem the sonic line does not attach to the body. Instead it moves up and attaches to the shock stem from the triple point. Also shown is the position of the contact surface which originates at the triple point.

The pressure distribution in the cells next to the surface of the body 1 after 1200 time steps is shown in Fig. 5. The pressure drops initially as the fluid expands from the stagnation point and then begins to increase due to the curvature change

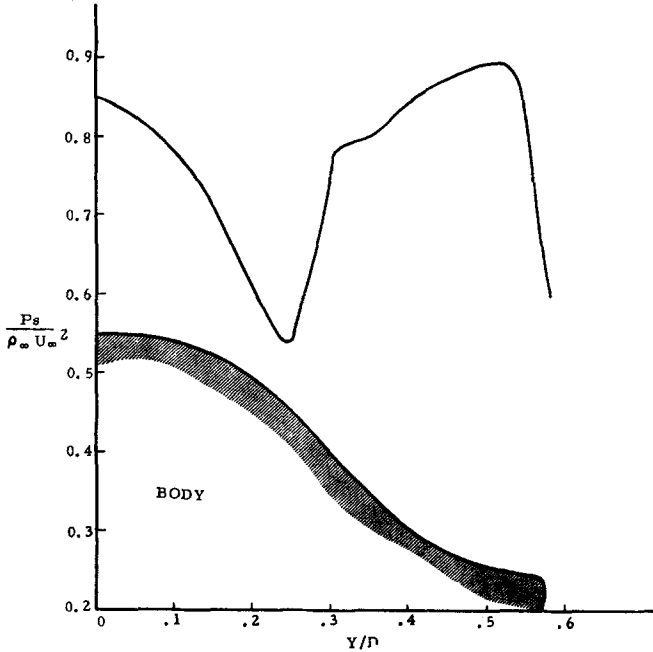


FIG. 5. Surface pressure on body 1 for mach 8 free stream after 1200 time steps.

of the body. This increase seems enhanced by a compression in the region where the triple point shock extends into the shock layer. Note that the pressure on the flare of the body appears to overshoot the nose stagnation pressure. The authors undertook a study of this phenomena to determine if it was physically correct or the result of artificial viscosity effect in the numerical scheme. The study unfortunately did not yield unquestionable evidence, but it did, however, produce results which suggest that the effect is real and not artificial. In summary the study revealed the following (1) overshoots or undershoots could not be produced with the Godunov difference method using one-dimensional test cases with large flow gradients and (2) the cells adjacent to the flare portion of the body receive the majority of fluid with a stagnation entropy lower than that of the normal shock stagnation condition.

The cells receive this fluid because streamlines emanating from non-normal portions of the bow shock collect very near the surface in the flare portion of the body. As a result the entropy of the fluid in the cell is less than stagnation entropy and consequently the maximum cell pressure can rise above the nose stagnation pressure. It is natural to expect a larger pressure overshoot for longer nosed bodies since streamlines of a lower entropy (from the region of small bow shock slope) will enter the surface cells on the flare. When the results of body 2 are discussed we will see that indeed this is the case.

Body 2 was a long nosed bell shape with the nose radius $5/100$ the base diameter. The body shape and the rays of the mesh are shown in Fig. 6. Also shown is the starting position of the smoothed bow shock used to start the final solution. This calculation served as a severe test of the computation procedure because of the sharp angle formed by the two branches of the bow shock at the triple point. As a

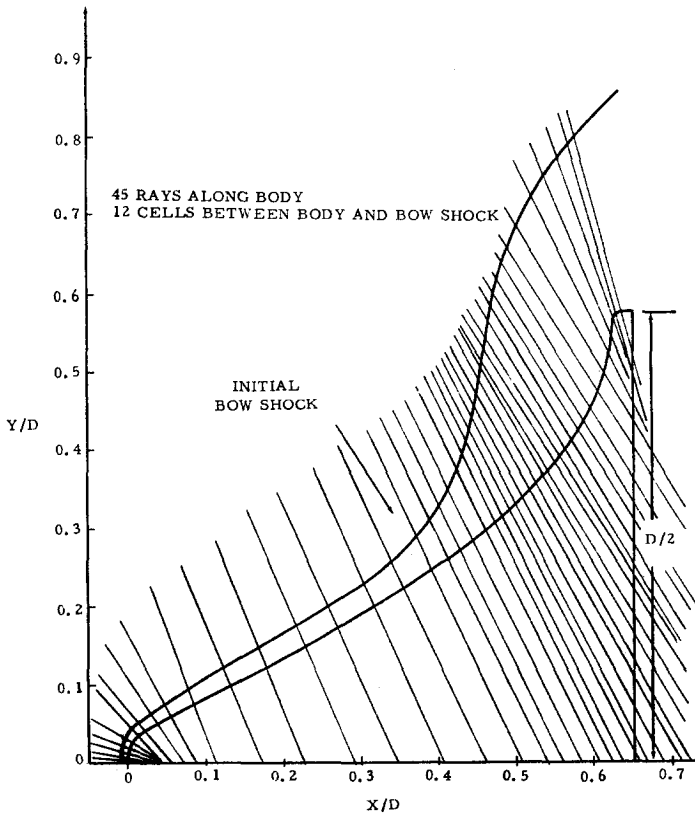


FIG. 6. Rays of mesh and initial bow shock shape for body 2.

result there was question as to whether the solution would reach a steady meaningful answer because of the difficulty in fitting the bow shock in this region. The calculation, however, approached a steady state at 1500 time steps after the shock shape of Fig. 6 was introduced. The resulting shock wave and sonic line patterns are shown in Fig. 7. The shock pattern looks acceptable except for the curvature of the upper branch of the bow shock near the triple point. Intuitively one would expect this shock to be approximately normal to the free stream instead of deflecting inward. Examination of Schlieren photographs from the work of Jones, Bushnell, and Hunt [11] indicate that indeed the shock wave in the physical problem is approximately normal. The error in the calculated shock position is due to the finite mesh size which does not permit the exact placement of the triple point nor proper account of the high curvatures of the shock stems. The sonic lines for body 2 are typical of a blunt body flow, but the contact surface near the triple point has a slight dip due to the shock curvature of the upper bow shock branch.

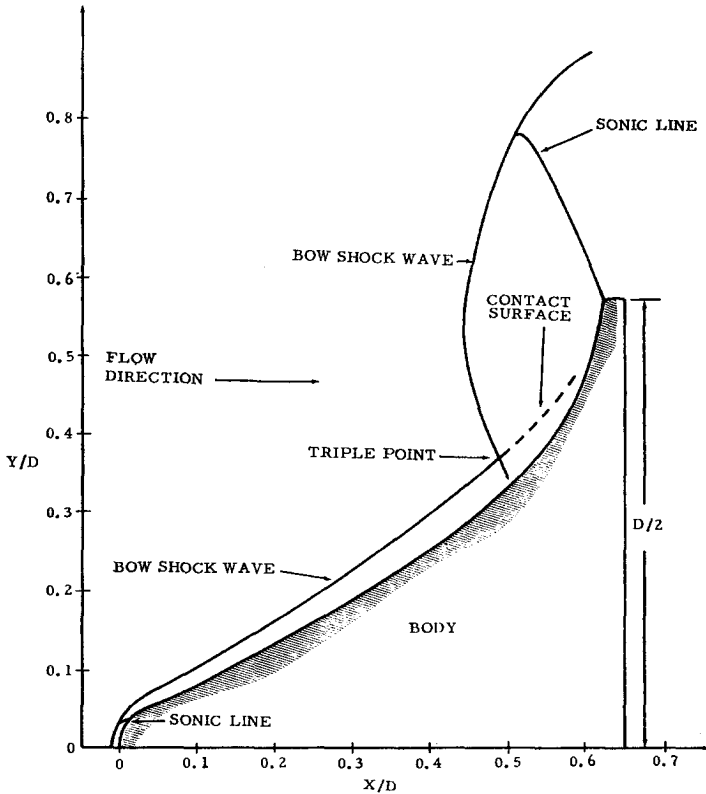


FIG. 7. Steady shock shapes and sonic lines for body 2 in mach 8.0 flow after 1500 time steps.

The surface pressure for the body is shown in Fig. 8 along with the experimental results of Jones, Bushnell, and Hunt [11]. Again the pressure overshoot on the flare is observed but as anticipated earlier, it is larger in magnitude than for body 1 even though the free stream conditions and body geometry of the flare of the body are exactly the same. The magnitudes of the calculated results seems to agree with the experiments, but are shifted down the body by the amount of the error in the triple point position. The experimental pressures indicate that the lower branch of the triple point shock strikes the body slightly ahead of the calculated position. An interesting comparison of pressures is obtained if one shifts the peak of the calculated pressure distribution to the approximate position it would have if the upper stem of the bow shock, near the triple point, were normal to the flow. Fig. 9 displays the result. In this situation the calculated results agree surprisingly well with the experiments. One other point of interest is that the calculated pressure distribution near the triple point shock does not exhibit random oscillations even though it was smeared. The smearing, however was, small since the jump was confined to two cells.

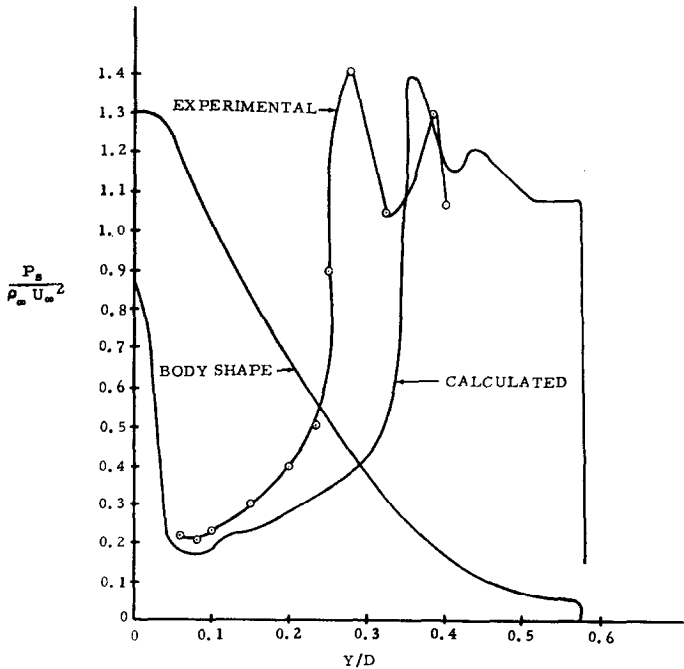


FIG. 8. Surface pressure on body 2 for mach 8.0 flow after 1500 time steps.

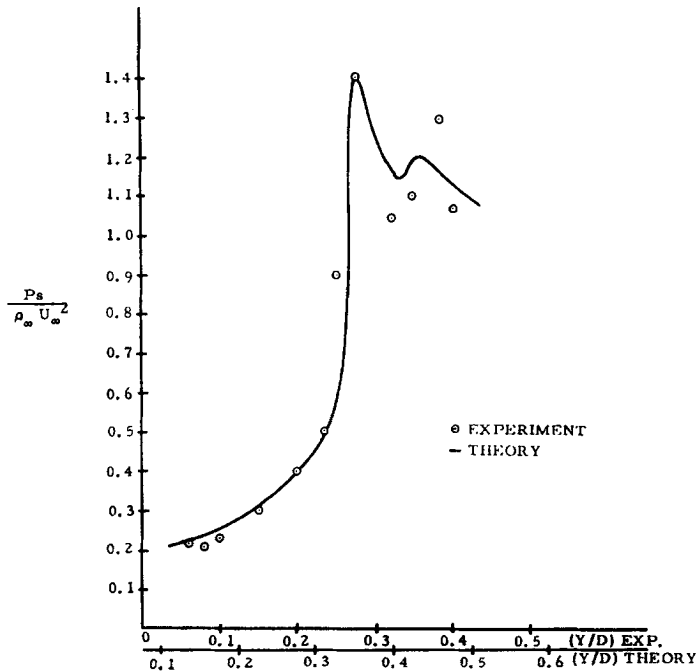


FIG. 9. Comparison of experimental and calculated surface pressures for body 2 with a shift in (Y/D) Coordinates for calculated results.

CONCLUDING REMARKS

The results of the calculations for the two bell-shaped bodies show the Godunov finite difference method to be stable during computation of bodies with strong compressions and large continuous changes in curvature. In addition the method computes triple point shock conditions reasonably well. The procedure seems limited only by the approximations introduced into the shock fitting analysis for the bow shock. Current analysis seems adequate as long as the angle between the two branches of the bow shock does not approach 90 degrees.

Calculation times required for the flow to reach a steady state were typically 15 to 20 minutes on a CDC 6600 computer for approximately 600 mesh points. In the physical problems this approximates the time required for the flow to travel 5 body lengths. For smooth bodies this time drops to about two body lengths.

In conclusion, the results of the calculations presented in this paper indicate that the Godunov method remains stable and yields reasonable results for most supersonic blunt-body flow situations, provided the analyst provides an adequate analysis of the flow conditions at the boundaries.

REFERENCES

1. D. LAX AND B. WENDROFF, Difference scheme for hyperbolic equations with high order accuracy, *Comm. Pure Appl. Math.* **17** (1964), 381.
2. Z. BURSTEIN, Numerical methods in multidimensional shocked flow, *AIAA J.* **2** (1964), 217.
3. V. V. RUSANOV, Supersonic flow around a blunt body, *J. Comput. Math. Math. Phys.*, (in Russian) **8** (1968), 616.
4. S. K. GODUNOV, Finite difference method for numerical computation of discontinuous solutions of the equations of fluid dynamics, *Mat. Sb.* **47** (89) (1959), 271; translated by I. Bohachevsky.
5. B. S. MASSON, T. D. TAYLOR, AND R. M. FOSTER, Application of Godunov's method to blunt body calculations, *AIAA J.* **7** (1969), 694.
6. G. MORETTI AND M. ABBOTT, A time dependent computational method for blunt body flows, *AIAA J.* **4** (1966), 2136.
7. A. A. DORODNITSYN, On a method for numerical solution of some aerohydrodynamic problems, *Proc. 3rd All-Sov. Math. Congr. II* (1956).
8. O. M. BELOTSEKOVSKII, On the calculation of flow past axisymmetric bodies with detached shock waves using an electronic computer, *J. Appl. Math. Mech.* **24** (1958), 745.
9. S. M. GILINSKY, G. F. TELENIN, AND G. P. TINYAKOV, A method for computing supersonic flow around blunt bodies accompanied by a detached shock wave, *Izv. Akad. Nauk SSSR Mekh. Mashinostr.* **4** (1964), 9.
10. S. K. GODUNOV, A. V. ZABRODIN, AND G. P. PROKOPOV, The difference schemes for two-dimensional unsteady problems in gas dynamics and the calculation of flows with a detached shock wave, English transl. *J. Comput. Math. Math. Phys., Acad. Sci. USSR* **1**, No. 6 (1961).
11. R. A. JONES, D. M. BUSHNELL, AND J. L. HUNT, Experimental flow field and heat transfer investigation of several tension shell configurations at a mach number of eight, NASA TN D-3800, 1967.
12. R. COURANT, K. O. FRIEDRICHS, AND H. LEWY, Über die Bartillen Differenzgleichungen der Mathematischen Physik, *Math. Ann.* **100** (1928), 32.